Langmuir

Article

pubs.acs.org/Langmuir

SiO_2@Au Core–Shell Nanospheres Self-Assemble To Form Colloidal Crystals That Can Be Sintered and Surface Modified To Produce pH-Controlled Membranes

Patricia Anne A. Ignacio-de Leon[†] and Ilya Zharov*

Department of Chemistry, University of Utah, Salt Lake City, Utah 84112, United States

ABSTRACT: We prepared colloidal crystals by self-assembly of gold-coated silica nanospheres, and free-standing nanoporous membranes by sintering these colloidal crystals. We modified the nanopore surface with ionizable functional groups, by forming a monolayer of L-cysteine or by surface-initiated polymerization of methacrylic acid. Diffusion experiments for the cationic dye Rhodamine B through L-cysteine-modified membranes showed a decrease in flux upon addition of an acid due to the nanopore surface becoming positively charged. Diffusion experiments for the neutral dye, ferrocenecarboxaldehyde, through the PMAA-modified membranes showed a 13-fold increase in flux upon addition of an acid resulting from the protonated polymer collapsing onto the nanopore surface leading to larger pore size. Our results demonstrate that SiO_2@Au core–shell nanospheres can self-assemble into colloidal crystals and that transport through the corresponding surface-modified Au-coated colloidal membranes can be controlled by pH.

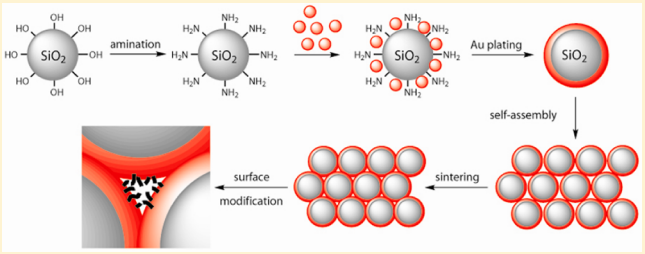

INTRODUCTION

Colloidal crystals made of metallic nanoparticles or coated with a metallic layer have been extensively investigated in the past decade because such structures possess properties suitable for applications in catalysis,[1,2] photonics,[3,4] surface-enhanced Raman spectroscopy (SERS),[5,6] and in chemical and biological sensors.[7,8] Two main strategies have been used to prepare these materials.[9−11] Metallic nanoparticles of various shapes have been assembled into the ordered structures directly, either by filtration[12] and evaporation[13] or by using an electric field-mediated assembly.[14−16] Polystyrene and silica colloidal crystals have been coated with metallic layers using layer-by-layer deposition of gold nanoparticles[17] or using a variety of dipping methods that utilized immobilization of metallic nanoparticles on the colloidal crystal surface and electroless plating.[6,8,18,19] An obvious alternative method for the preparation of the latter materials is the self-assembly[20] of metal–shell dielectric-core nanoparticles into the ordered close-packed face-centered (fcc) lattice. However, to the best of our knowledge, this approach has not been previously reported. In the present article, we demonstrate that SiO_2@Au core–shell nanospheres can indeed self-assemble into the ordered colloidal crystals.

In addition to the aforementioned applications, introducing the gold surface into the ordered colloidal structures may lead to novel nanoporous materials, which is important when developing new membranes.[21,22] Currently, most membrane separations are performed using polymeric membranes,[23] whose disadvantages include low porosity and limited compatibility with organic solvents. Alternative membrane materials include nanoporous zeolites,[24] silicon nitride,[25] mesoporous silica,[26] anodized alumina,[27,28] nanotubes,[29,30] and silicon.[31] While possessing high stability and porosity, most of these materials contain cylindrical nanopores. In contrast, membranes that contain convoluted pores have higher separation efficiency.[32] Thus, silica colloidal crystals provide an attractive membrane material because of their highly porous inorganic structure with interconnected nanoscale tetrahedral and octahedral voids between the neighboring spheres that provide tortuous pathways for molecules diffusing through the crystal.

Recently, we have prepared free-standing silica colloidal membranes by sintering silica colloidal crystals.[33] While much thicker compared to ultrathin inorganic membranes,[31] they possess high molecular flux and size selectivity.[34] We also showed that pH and ion-responsive free-standing silica colloidal membranes can be prepared by their surface modification with polyelectrolyte brushes.[35]

Using SiO_2@Au core–shell nanospheres to prepare free-standing colloidal membranes may provide two advantages. First, sintering as a method of preparing free-standing silica colloidal membranes results in the loss of the silanol surface functionality at high temperature, requiring rehydroxylation if further surface modifications are desired. Using gold on the surface of the nanospheres comprising the colloidal membranes might eliminate the need for surface reactivation. Second, it would introduce new types of nanopore surface functionalization based on thiol–gold chemistry. The current article describes the sintering of colloidal crystals obtained by the

Received: October 13, 2012
Revised: February 8, 2013
Published: February 11, 2013

self-assembly of gold-coated silica nanospheres as well as the surface modification of the resulting free-standing membranes with L-cysteine and poly(methacrylic acid), PMAA, to obtain pH-controlled transport through these membranes.

While the gold-coated colloidal nanoporous membranes have not been reported previously, the selective molecular transport through cylindrical gold-coated nanopores has been described earlier for track-etched polycarbonate membranes. A gold surface modification with a self-assembled monolayer (SAM) of L-cysteine[36] or 11-mercaptoundecanoic acid[37,38] resulted in pH-switchable transport selectivity for ions and proteins.[39] Comparison of the performance of membranes modified with perfluorodecanethiol or its alkyl analogue 1-decanethiol[40] and with hexadecanethiol or 1-mercaptoethanol[41] showed transport selectivity for hydrophobic molecules. In addition to the above small molecule modifiers, polymers such as polypeptides[42] and polyelectrolytes[43] have also been grafted onto the Au-coated nanopores.[44] Thermally switchable and size-selective transport of dye-labeled dextrans through gold-coated nanopores with surface-grafted poly(*N*-isopropylacrylamide) (PNIPAAm) chains[45] and size-exclusion protein separations using poly(ethylene glycol) (PEG) to minimize protein adsorption[46] have been reported.

EXPERIMENTAL SECTION

Materials. Ammonium hydroxide (28−30% as NH_3, EMD Chemicals, Inc.), tetrabutylammonium hydroxide (40 wt % solution in water, Sigma-Aldrich), triethylamine (J.T. Baker), hydroxylamine hydrochloride (Sigma-Aldrich), sodium hydroxide (Mallinckrodt Chemicals), sodium carbonate anhydrous (Mallinckrodt Chemicals), sodium bicarbonate (Mallinckrodt Chemicals), sodium nitrate (J.T. Baker), ammonium chloride (Mallinckrodt Chemicals), magnesium sulfate anhydrous (Mallinckrodt Chemicals), (ethylenedinitrilo)-tetraacetic acid disodium salt dihydrate (Mallinckrodt Chemicals), bromine solution (EMD Chemicals, Inc.), dichloromethane (Mallinckrodt Chemicals), nitric acid (68−70%, ACS grade, EMD Chemicals, Inc.), trifluoroacetic acid (Acrōs), tetraethyl orthosilicate (99.999+%, Alfa Aesar), ethanol (200 proof, ACS grade, Pharmaco-Aaper), tetrachloroaurate(III) trihydrate (Acrōs Organics), sodium citrate dihydrate (Alfa Aesar), sodium borohydride (Alfa Aesar), sodium methacrylate (Alfa Aesar), copper(I) bromide (Aldrich), copper(II) bromide (Aldrich), 2,2′-dipyridyl (Aldrich), 11-mercapto-1-undecanol (Aldrich), 2-bromoisobutyryl bromide (Aldrich), L-cysteine (Aldrich), dihexadecyl disulfide (Aldrich), ferrocenecarboxaldehyde (Aldrich), and Rhodamine B (Sigma) were all used as received. Nanobead NIST Traceable Particle Size Standards (40 and 80 nm) were obtained from Polysciences, Inc. Millipore water (18 MΩ·cm) used in all experiments was obtained from a Barnstead "E-pure" water purification system. Acetonitrile (HPLC grade, VWR Scientific) was freshly distilled from calcium hydride. Column chromatography was performed using silica gel (40−63 μm) with 60 Å pore diameter (Silicycle Chemical Division). TLC was performed using Silica gel 60 F_{254} on aluminum sheets (EMD Chemicals, Inc.). All glassware was cleaned with Millipore water prior to use. Scanning electron microscopy (SEM) images were obtained using either a Hitachi S3000-N or an FEI NanoNova instrument. Transmission electron microscopy (TEM) images were obtained using an FEI Philips Tecnai T-12 or a Tecnai F30 instrument. UV/vis/NIR absorbance measurements were collected using an Ocean Optics USB2000 or USB4000 instrument or a PerkinElmer Lambda 750 instrument. A Branson 1510 sonicator was used for all sonications. A Clay Adams Compact II Centrifuge (3200 rpm, Becton Dickinson) was used for all centrifugations. A Fisher Scientific Isotemp Programmable Muffle Furnace (Model 650) was used for all sintering purposes. All zeta-potential measurements were carried out in water using a NICOMP 380 ZLS zeta-potential/particle sizer (PSS-NICOMP Particle Sizing Systems). Thermogravimetric analyses were performed using a TA Instruments TGA 2950 thermogravimetric analyzer.

Preparation of Silica Spheres. Silica spheres were prepared according to the modified literature procedures.[47,48] A batch of silica spheres was prepared by mixing 500.0 mL of an ethanolic solution containing TEOS (51.4 mL, 0.20 mol) with 500.0 mL of an ethanolic solution containing NH_4OH (70.0 mL, 1.1 mol) and water (257 g, 14.3 mol). These two solutions were poured simultaneously into a 2 L Erlenmeyer flask and vigorously stirred. The resulting mixture had final concentrations of 0.2 M TEOS, 1.1 M NH_3, and 17.0 M H_2O. The onset of turbidity after a short while indicated the start of silica sphere formation. After 24 h, the resulting solution was poured into 15 mL centrifuge tubes (Corning) and centrifuged for 10 min. The supernatant was discarded, leaving the spheres as pellets at the bottom of the centrifuge tubes. Purification of the spheres was achieved by a repetitive cycle of suspending the spheres by 10 min sonication followed by centrifugation for 10 min in a series of 10 mL supernatants: 100% water, 25% ethanol, 50% ethanol, 75% ethanol (twice), and 100% ethanol. After the final rinsing, the supernatant was decanted and the silica spheres air-dried overnight. The dried spheres were then preshrunk by transferring to a Petri dish (breaking any large aggregates with a spatula) and placing in a furnace programmed to heat the spheres for 4 h at 600 °C[49−51] (the desired temperature achieved at a heating rate of 20 °C/min). SEM images were obtained for the spheres, and their size was determined from 100 individually measured spheres to be 350 ± 20 nm in diameter.

Preparation of Au Nanoparticles. Gold nanoparticles of nominal 3 nm size were prepared according to the literature procedure.[18] Briefly, 90.0 mL of a 0.27 mM $HAuCl_4{\cdot}3H_2O$ aqueous solution was mixed with 2.0 mL of 1% sodium citrate aqueous solution with stirring. After 1 min, 1.0 mL of freshly prepared 0.075% $NaBH_4$ in 1% sodium citrate solution was added, and the mixture stirred for another 5 min. The reaction temperature was maintained at 4 °C. This stock solution of Au nanoparticles was then stored in the refrigerator. TEM images indicated that the nanoparticles were prone to aggregation, leading to aggregates with sizes ranging from about 8 to 40 nm in diameter.

Preparation of Silica-Core Au-Shell (SiO_2@Au) Spheres. The preshrunk particles were aminated prior to Au-coating. To 13.3 g of silica spheres dispersed in 200 mL of dry acetonitrile, 0.40 mL of 3-aminopropyltriethoxysilane was added, and the mixture was vigorously stirred under N_2(g) overnight. The aminated particles were isolated by repeated centrifugation and resuspension in acetonitrile, tetrahydrofuran, xylene, twice in water, and twice in acetonitrile, followed by air-drying. The aminated spheres were then immersed in an aqueous solution of the Au nanoparticles (diluted 6-fold from the stock solution) for 10 h with stirring. The wine red color of the solution disappears as the Au nanoparticles adsorbed onto the surface of the spheres. The faintly pink spheres were then collected via centrifugation and washed by sonication in deionized water at least three times prior to air-drying.

The spheres were ground up and placed into a 250 mL Erlenmeyer flask, to which 200 mL of a Au-plating solution (0.1% w/w $HAuCl_4$ in 0.40 mM $NH_2OH{\cdot}HCl$) were added with vigorous stirring that continued for 30 min. The colloidal solution color turned a deep purple as Au shells were chemically deposited onto the surface of the silica spheres. The Au-coated spheres were collected in 15 mL Corning tubes, centrifuged, and rinsed repetitively with deionized water at least five times. The modified spheres were dried under a stream of N_2(g) to give a purple powder. TEM images (Figure 1) confirmed the formation of an Au coat of uniform thickness and relatively smooth surface around the silica spheres. The thickness of the Au shell was estimated to be ∼25 nm based on comparison of SEM images of aminated and Au-coated particles.

Preparation of Free-Standing Membranes. First, colloidal crystals (Figure 3A) were prepared by vertical deposition onto a glass substrate from 12 to 15 wt % colloidal solutions of Au-coated silica spheres in ethanol. The resulting crystals were then gently lifted from the glass slides and sintered in a furnace for 10 h at 1000 °C (the desired temperature achieved at a heating rate of 5 °C/min). The

dx.doi.org/10.1021/la304069x | *Langmuir* 2013, 29, 3749−3756

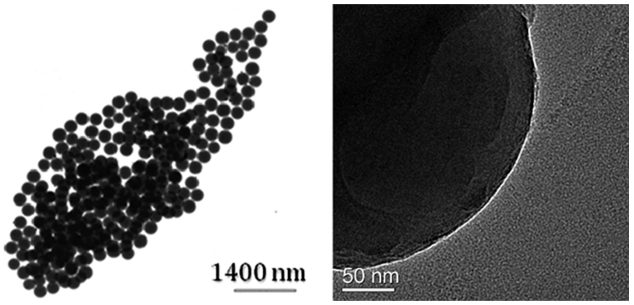

Figure 1. Representative TEM images of Au-coated silica spheres prepared in this work.

sintered colloidal membranes were now noticeably much more robust and durable, making handling easier. SEM images of the membranes (Figure 3B) were obtained to give an average diameter of 320 ± 10 nm as measured from 100 individual spheres in the colloidal membrane. The thickness of each colloidal membrane was measured with a Vernier caliper at six points throughout the piece and used when calculating molecular flux. The average thickness of the membranes was 0.6−0.8 mm. For diffusion measurements, the sintered membranes were sandwiched between two PTFE washers (5.0 mm i.d., 14.0 mm o.d., and 1.0 mm thickness, Small Parts, Inc.) with Loctite Hysol 0151 Epoxy. Membranes constructed this way were allowed to cure for at least 24 h prior to use in diffusion experiments.

Surface Modification with L-Cysteine. L-Cysteine chemisorption onto the Au surface was performed according to the literature procedure.[36] Briefly, sintered membranes of Au-coated silica spheres were immersed in a 2 mM solution of L-cysteine in 80% ethanol for 24 h with stirring in an inert atmosphere. The membranes were then rinsed with ethanol and dried in the air.

Surface Modification with *n*-Hexadecyl Disulfide. A SAM of hexadecanethiol was chemisorbed onto the Au-coated nanopores by immersing the sintered membranes in a 2 mM solution of dihexadecyl disulfide in 1-octanol for 24 h with stirring in an inert atmosphere. The membranes were then rinsed with copious amounts of ethanol and air-dried.

Synthesis of ATRP Initiator. The polymerization initiator was synthesized according to a previously reported procedure.[52] Briefly, the initiator precursor was prepared by dissolving 1.0225 g of 11-mercapto-1-undecanol in 37.5 mL of dichloromethane and 5 mL of 10% $KHCO_3$ solution in a round-bottom flask with stirring, to which 128 μL of bromine solution was added dropwise. After the brown color of bromine had disappeared, the aqueous phase was extracted with 50 mL of dichloromethane. The organic phases were combined and dried with anhydrous $MgSO_4$. Solvent removal yielded a white solid (average 56.8% yield) whose ^{1}H NMR spectrum was in agreement with that reported in the literature. To 1.25 g of the disulfide precursor dissolved in 75 mL of dichloromethane, 2.09 mL of triethylamine was added, and the mixture was cooled to 0 °C under an inert atmosphere. The resulting solution was stirred for 1 h after 0.94 mL of 2-bromoisobutyryl bromide was added dropwise. The temperature was then brought to 25 °C, and stirring continued for another 2 h, after which the solution was extracted with 2 N Na_2CO_3 saturated with NH_4Cl. The organic solvent was evaporated to afford a pale yellow viscous liquid. The crude product was purified by flash chromatography using 1:1 dichloromethane/acetonitrile mixture as a mobile phase. The final product was a viscous, clear yellow liquid (average 65.9% yield) whose ^{1}H NMR spectrum was in good agreement with that reported previously for the initiator.

Surface Modification with Polymer Brushes. Poly(methacrylic acid), PMAA, brushes were grown on the surface of the Au by atom-transfer radical polymerization.[53] The substrates (either Au-coated spheres or Au-coated sintered membranes) were submerged in 1 mM initiator solution in absolute ethanol overnight in a nitrogen atmosphere, after which the substrates were rinsed with ethanol and air-dried. In a N_2(g)-filled flask, 2.12 g (20 mmol) of sodium methacrylate, 28.7 mg (0.20 mmol) of CuBr, 9.0 mg (0.04 mmol) of $CuBr_2$, and 78.4 mg (0.48 mmol) of 2,2′-dipyridyl were mixed with 4 mL of deionized water (pH 9, purged with N_2(g) for at least 30 min beforehand) with stirring at room temperature for ∼5 min. The initiator-modified Au-coated substrates were then added into the flask, and the polymerization was carried out at room temperature. The polymerization time was varied from 5 to 25 min for the suspended spheres and up to 45 min for the sintered membranes. The substrates were then washed with deionized water, sonicated in 0.1 M EDTA solution, rinsed with water and ethanol, and N_2(g)-dried.

Diffusion Measurements. Diffusion through the colloidal membranes was studied by placing a membrane between two connected 1 cm quartz cuvettes. The feed cell contained 4.00 mL of an aqueous dye solution while the reservoir cell contained 4.00 mL of water. The membrane was placed between two Kalrez O-rings to prevent leaking, and the whole assembly was then secured with a clamp. Each cell was covered with Parafilm to prevent evaporation, and the contents of both cells were continually stirred. The reservoir cell was placed between two fiber-optic cables, and the flux was monitored by recording the absorbance in the reservoir cell for at least 18 h. The absorbance was measured at λ_{max} (488 nm for ferrocenecarboxaldehyde and 546 nm Rhodamine B). Data points were acquired every 150 s with an initial delay of 150 s. Each diffusion experiment was performed in triplicate. Prior to using a membrane for a new experiment, it was immersed in deionized water for at least 2 days, and the water was replaced occasionally to ensure the complete removal of the dye from the membrane.

RESULTS AND DISCUSSION

Preparation of Free-Standing Au-Coated Membranes. To prepare Au-coated silica spheres, amine groups were first introduced onto the surface of 316 nm silica spheres, resulting in a thin polymeric layer of silamines. The amine groups acted as ligands for the chemisorption of small (2−10 nm diameter) gold nanoparticles, which in turn served as nucleation sites that, upon immersion of the nanoparticles in a gold-plating solution, grew larger and eventually coalesced to form an Au coat of uniform thickness around each silica sphere. TEM images showed that the gold-coated silica nanoparticles retained a uniform spherical shape (Figure 1). High-resolution Z-contrast images of the nanospheres in bright field showed a lighter outer area of about 25 nm thickness corresponding to the Au layer. Each of the modifications described above was followed by the changes in color of the colloidal solutions and by DLS, SEM, and TEM (Table 1). The UV/vis/NIR absorbance spectra for

Table 1. Summary of Measured Diameters for the Prepared Silica Nanoparticles

	diameter, nm	
particles	DLS	SEM
as-made	365 ± 40	350 ± 20
preshrunk	368 ± 40	316 ± 20
amine-modified	361 ± 40	317 ± 20
with adsorbed Au NPs	389 ± 40	323 ± 20
Au-coated	443 ± 40	338 ± 10
sintered membrane		320 ± 10

unmodified and Au-coated silica spheres (Figure 2) showed intensified absorption bands near 1900 and 3000 nm that can be attributed to the presence of the Au shell around the silica core. We believe that the peak near 3000 nm is indicative of continuous surface coverage with Au, in agreement with increasingly red-shifted absorbance bands as the size approaches that of bulk Au. There is also an apparent increase

dx.doi.org/10.1021/la304069x | Langmuir 2013, 29, 3749−3756

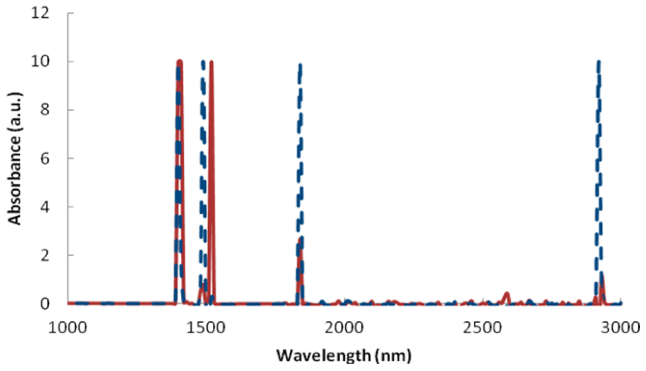

Figure 2. UV/vis/NIR absorbance spectra of bare silica (red solid line) and Au-coated silica (blue dashed line) spheres.

in the intensity of the band at 1480 nm while the absorbance at 1500 nm decreased in intensity.

Colloidal crystals were prepared next by the vertical deposition from colloidal solutions of Au-coated silica spheres. Coating the silica spheres with a gold shell did not affect the self-assembly of the spheres into an fcc arrangement (Figure 3A), although it is not defect-free. Free-standing membranes

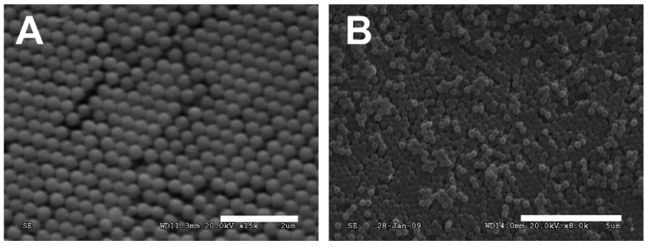

Figure 3. SEM images of (A) self-assembled and (B) sintered SiO_2@Au colloidal membranes. Scale bar is 2 μm in (A) and 5 μm in (B).

(Figure 3B) were then produced by sintering the self-assembled material at 1000 °C. Sintering led to the decrease in the nanosphere diameter, from 338 to 320 nm. Thus, the nanopore "radius" (the distance from the center of the nanopore projection to the nearest sphere surface) in the resulting Au-coated membranes was 24 nm. In addition to providing mechanical integrity and strength to the membrane, sintering at 1000 °C also ensured a uniform Au coverage necessary for subsequent surface functionalizations with SAMs. Indeed, it has been reported[54] that temperatures as low as 325 °C are sufficient to cause surface melting of gold. Sintering, while distorting the top layer of Au-coated membranes, did not appear to affect the fcc packing of the inner layers of the colloidal crystal (Figure 3B). The sintered membranes showed a stop band at ca. 650 nm measured by light microscopy in the reflectance mode.

In order to investigate the integrity of the sintered Au-coated membranes, we performed both diffusion and size-exclusion experiments using 40 and 80 nm polystyrene nanospheres. We found that while 40 nm nanospheres can diffuse through the sintered membranes and are not retained in the pressure-driven separation, 80 nm nanospheres do not diffuse through these membranes and are separated out. This confirmed that sintered membranes with 48 nm nanopore "diameter" contain no mechanical defects.

Membranes Surface-Modified with L-Cysteine. In order to demonstrate that the sintered Au-coated membranes can be surface-modified with a self-assembled monolayer (SAM) of thiol-containing molecules, we treated the membranes with L-cysteine (Figure 4A) by soaking them in 80% ethanolic solution

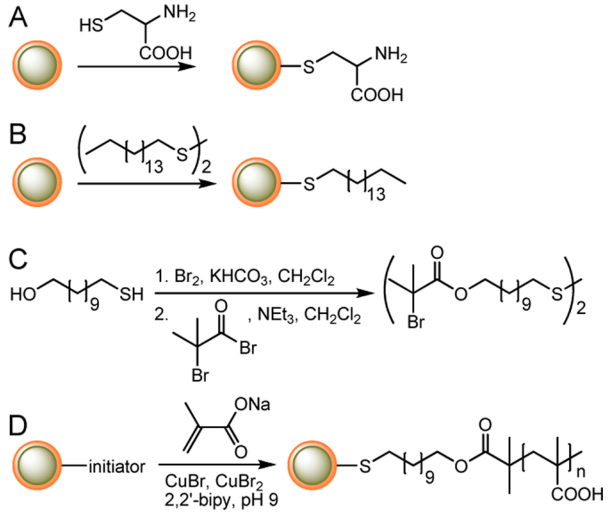

Figure 4. Reaction schemes for surface modification of the Au-coated SiO_2 spheres: (A) formation of a SAM of L-cysteine; (B) formation of a SAM of hexadecanethiol; (C) synthesis of the initiator molecule for (D) the ATRP of PMAA.

of L-cysteine.[36] The nanoporous nonflat membrane is difficult to analyze for the presence of surface molecules. Therefore, we recorded the IR spectrum of the Au-coated silica spheres surface-modified with L-cysteine as a model for the Au-coated membrane surface modification. We found a 1735 cm^{-1} band in the IR spectrum (Figure 5) corresponding to a carbonyl stretch, which confirmed the presence of L-cysteine on the surface.

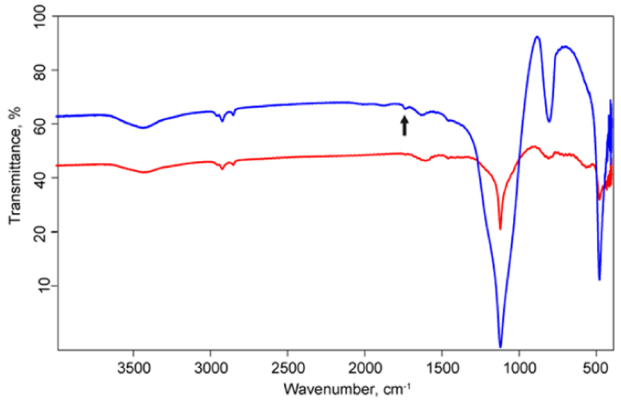

Figure 5. FT-IR spectra of unmodified (red) and L-cysteine-modified (blue) Au-coated silica spheres.

To determine whether the L-cysteine surface modification of Au-coated colloidal membranes would lead to the charge-selective molecular transport, we studied the concentration gradient-driven diffusion of a cationic dye, Rhodamine B, by measuring the diffusion rate R_D (mol s^{-1}) through a membrane of a known area S (cm^2). Knowing the value of R_D allowed for the calculation of the molecular flux $J_{colloid}$ (mol s^{-1} cm^{-2}) through the membrane (eq 1).

$$R_D = J_{colloid} S \quad (1)$$

dx.doi.org/10.1021/la304069x | Langmuir 2013, 29, 3749−3756

A solution for Fickian diffusion (eq 2) was then used to determine the diffusion coefficient $D_{colloid}$ ($cm^2\ s^{-1}$) of the dye as it traverses through the colloidal membrane of thickness L with void fraction ε of 0.26 and tortuosity τ of 3.0:[55]

$$J_{colloid} = \frac{\Delta C}{L}\frac{\varepsilon}{\tau}D_{colloid} \quad (2)$$

We measured the number of moles of a dye molecule that diffused through the membrane as a function of time in a diffusion cell apparatus described elsewhere.[33] The measurements were performed at pH 7 and 1.5. Upon addition of the acid, the diffusion rate decreased. Both the amine and carboxylate groups in L-cysteine become protonated at low pH, resulting in a positively charged nanopore surface. Thus, the observed change in the calculated $D_{colloid}$ value (Table 2) should be due to the electrostatic repulsion between the cationic dye and the nanopore surface. The observed change in $D_{colloid}$ is small (the ratio of $D_{colloid}$ in the absence and presence of trifluoroacetic acid is only 1.3) and similar to the results obtained for amine-modified free-standing silica colloidal membranes.[33] This may be due to the low surface coverage of the nanopores with L-cysteine, which is supported by the low intensity of the carbonyl peak in the IR spectrum as well as negligible percent weight loss in thermogravimetric analysis (TGA).

Table 2. Calculated Average Diffusion Coefficients for Rhodamine B through L-Cysteine and *n*-Hexadecyl-Modified Au-Coated Colloidal Membranes[a]

	$D_{colloid}$ ($cm^2/s \times 10^{-6}$)		
membrane modified with	pH 7	pH 1.5	selectivity
L-cysteine	3.6 ± 0.3	2.9 ± 0.2	1.3
n-hexadecyl	3.5 ± 0.1	3.6 ± 0.3	1.0

[a]Selectivity was calculated as the ratio of coefficients without and with TFA.

To confirm that the above observations result from the electrostatic effects, we modified the nanopore surfaces with a nonionizable moiety, a 16-carbon *n*-alkyl chain of hexadecanethiol (Figure 4B). Diffusion experiments of Rhodamine B through the alkyl-functionalized membranes (Figure 6) indeed showed no difference in calculated diffusion coefficients in the absence and presence of the acid (Table 2).

Membranes Surface-Modified with PMAA. We explored another type of surface modification for Au-coated colloidal membranes, which allows manipulating their effective nanopore size. We used polyelectrolyte brushes of poly(methacrylic acid), PMAA, formed on the gold surface of the colloidal nanopores by atom-transfer radical polymerization (ATRP) from initiators bound to the gold surface through the thiol chemistry.

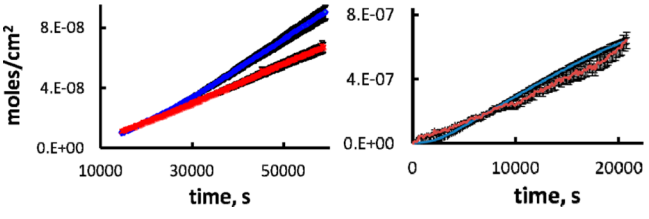

Figure 6. Representative plot of the molecular flux of Rhodamine B through L-cysteine-modified membranes in the absence (blue) or presence (red) of TFA (left) and through *n*-hexadecyl-modified membranes in the absence (blue) or presence (red) of TFA (right).

In order to confirm that ATRP of methacrylate can be performed on the surface of SiO_2@Au core–shell nanospheres, they were suspended in solution and modified with the initiator moiety (Figure 4C) followed by the treatment with sodium methacrylate in the presence of a copper(I) catalyst (Figure 4D). TEM images of the modified nanoparticles (Figure 7) that were rigorously washed by sonication confirmed the presence of the organic polymer that was covalently bound to the surface. The polymer growth as a function of polymerization time was monitored by DLS and TGA, and the polymer brush length and degree of polymerization n were calculated. The results of these measurements are shown in Table 3. The TGA plots (Figure 8) show increasing percent weight loss with increasing ATRP time. The weight loss around 240–250 °C can be attributed to the initiator decomposition, while PMAA is lost from 375 to 420 °C (Figure 8). The DLS data (Table 3) also support the notion that longer polymer brushes are formed with longer polymerization time. The absolute polymer brush length determined by DLS is significantly larger than that

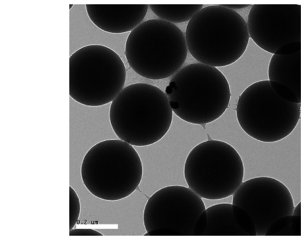

Figure 7. Representative TEM image of SiO_2@Au spheres with PMAA grown for 30 min (scale bar = 200 nm).

Table 3. DLS and TGA Data for PMAA-Modified SiO_2@Au Spheres

particles	DLS brush length, nm	TGA polymer brush[a]
initiator-modified		6.75 initiators/nm^2
5 min ATRP	20	*n* = 30; 9 nm
10 min ATRP	39	*n* = 33; 10 nm
15 min ATRP	81	*n* = 43; 12 nm

[a]The calculated polymer brush lengths based on TGA data were obtained with the assumption that all initiators reacted to grow PMAA, estimated 1.7 nm length of the initiator moiety, and 0.25 nm length of each monomer unit.

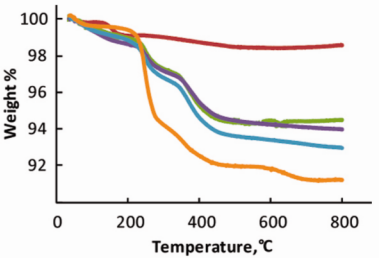

Figure 8. TGA of initiator-modified (red) SiO_2@Au spheres with PMAA grown from the surface for 5 min (green), 10 min (purple), 15 min (blue), and 25 min (orange) polymerization times.

dx.doi.org/10.1021/la304069x | *Langmuir* 2013, 29, 3749–3756

estimated by TGA, which is the result of DLS measuring the hydrodynamic radius of the nanoparticles with PMAA brushes swollen in water.

Next, we prepared PMAA-modified Au-coated membranes by ATRP. The sintered substrates were first modified with a SAM of the initiator; its surface density determined by TGA was 0.74 molecule/nm^2 (Table 4), lower than that found for the initiator-modified SiO_2@Au core−shell nanospheres prepared in solution (Table 4). The membranes were then soaked in a mixture of the methacrylate monomer and copper(I) catalyst for various amounts of time. An SEM image of the PMAA-modified membrane is shown in Figure 9

Table 4. TGA Data for PMAA-Modified Au-Coated Membranes

membrane	TGA polymer brush[a]
initiator-modified	0.74 initiators/nm^2%
45 min ATRP	n = 41; 12 nm

[a]The calculated polymer brush length based on TGA data was obtained with the assumption that all initiators reacted to grow PMAA, estimated 1.7 nm length of the initiator moiety, and 0.25 nm length of each monomer unit.

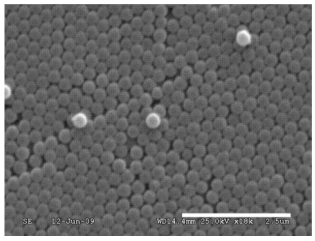

Figure 9. Representative SEM image of a sintered SiO_2@Au membrane with PMAA grown for 10 min (scale bar = 2.5 μm).

and demonstrates that the crystal order and porosity are preserved after the polymerization. TGA of the resulting membranes confirmed the formation of the polymer inside the nanopores. For example, after 45 min of ATRP the polymer chains containing 41 monomer units were formed (Table 4), comparable to the polymer brush obtained on SiO_2@Au core−shell nanospheres in solution after 15 min of ATRP (Table 3).

PMAA is an environmentally responsive polymer that possesses various degrees of swelling depending on pH.[56,57] To determine if PMAA polymer brushes inside the nanopores of Au-coated colloidal membranes respond to variations in pH, we studied the diffusion of a neutral dye, ferrocenecarboxaldehyde, Fc(CHO), through the membranes as a function of pH (Figure 10), so that any changes in the molecular flux could be attributed exclusively to the changes in the polymer conformation and not to electrostatic interactions between PMAA chains and the diffusing species. Diffusion rates of Fc(CHO) through PMAA-modified membranes (Table 5) decreased with increasing length of the polymer chains inside the nanopores, which is due to the decrease in the effective size of the nanopores as they become partially blocked with the polymer brushes. Comparison of the calculated $D_{colloid}$ values for the unmodified and polymer-modified membranes showed that diffusion was hindered by a factor of 7.6 after 30 min of polymerization. We did not observe complete blockage of the nanopores even after 45 min of polymerization, as the

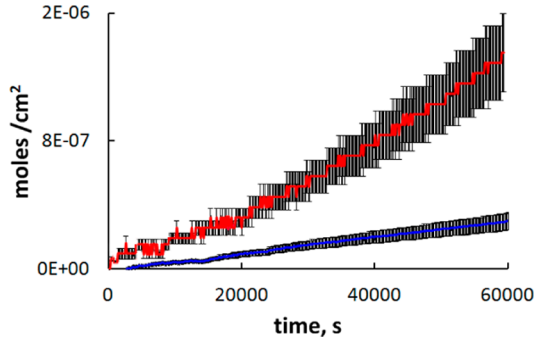

Figure 10. Representatibve plots of the molecular flux of ferrocene carboxaldehyde through the SiO_2@Au membranes modified with PMAA via ATRP for 45 min (with TFA, red; without TFA, blue).

Table 5. Calculated Average Diffusion Coefficients for Ferrocenecarboxaldehyde through PMAA-Modified Gold-Coated Silica Colloidal Membranes[a]

	$D_{colloid}$ (cm^2/s ×10^{-6})		
ATRP time (min)	without TFA	with TFA	selectivity
10	6.7 ± 0.6	16 ± 2	2.4
30	0.9 ± 0.2	12 ± 2	13
45	0.9 ± 0.3	10 ± 3	12

[a]Selectivity was calculated as the ratio of coefficients with and without acid.

calculated D_{eff} values for the membranes modified for 30 and 45 min were similar. It is possible that the polymerization reaction slows down considerably after 30 min.

Upon addition of 50 mM trifluoroacetic acid to the diffusing solution, we observed an increased flux of Fc(CHO) through the membranes (Table 5). This is consistent with the known behavior of PMAA in response to the pH changes.[56,57] In the absence of TFA, the polymer brushes are extended because of a significant degree of dissociation of the −COOH groups. Indeed, the pH 7 of the neutral solution is higher than the pK_a ∼ 5 of PMAA.[58] In the presence of TFA, deprotonation along the chain is suppressed, electrostatic repulsions are minimized, and thus the polymer brushes undergo deswelling. The PMAA chains fold and collapse onto the gold surface, thus leading to larger nanopores. The calculated selectivities, obtained as the ratio of $D_{colloid}$ in the presence and absence of the acid (Table 4), showed that the pH response of the PMAA-modified nanopores depends on the polymer brush length. The permselectivity was only 2.4 for the Au-coated membrane after 10 min of polymerization, but increased to 13 for the membranes obtained after 30 min of polymerization, and did not change for the membrane after 45 min of polymerization. The latter observation is consistent with the notion that the polymer length does not increase after 30 min of polymerization, as discussed above. That the steric effect was more pronounced for longer PMAA chains is likely due to the increased steric blocking of the nanopores. The pH-controlled permselectivity observed for the PMAA-modified Au-coated colloidal membranes is similar to that found for silica colloidal membranes surface-modified with pH- and temperature-responsive polymers.[35,59,60]

CONCLUSIONS

We demonstrated that colloidal crystals can be formed by self-assembly of gold-coated silica spheres, and free-standing

dx.doi.org/10.1021/la304069x | Langmuir 2013, 29, 3749−3756

colloidal membranes can be prepared by sintering these colloidal crystals. We also showed that the nanopore surface of these membranes can be modified with various organic moieties by the SAM formation or by surface-initiated polymerization. We found that the transport through the nanopores in Au-coated colloidal membranes modified with *n*-alkyl chains is not affected by changes in pH, while the diffusion rates for a cationic species through L-cysteine-modified nanopores decreased in the presence of an acid due to electrostatic effects. We also found that the transport in the PMAA-modified Au-coated membranes is pH-responsive, as the diffusion rates of a neutral species increased with decreasing pH.

AUTHOR INFORMATION

Corresponding Author

*E-mail: i.zharov@utah.edu.

Present Address

[†]Chemical and Biological Engineering Department, Northwestern University, 2145 Sheridan Road, Evanston, IL 60208.

Notes

The authors declare no competing financial interest.

ACKNOWLEDGMENTS

This work was supported by the National Science Foundation (MWN grant DMR-1008251).

REFERENCES

(1) Wakayama, H.; Setoyama, N.; Fukushima, Y. Size-Controlled Synthesis and Catalytic Performance of Pt Nanoparticles in Micro- and Mesoporous Silica Prepared Using Supercritical Solvents. *Adv. Mater.* **2003**, *15*, 742−745.

(2) Li, H.; Wang, R.; Hong, Q.; Chen, L.; Zhong, Z.; Koltypin, Y.; Calderon-Moreno, J.; Gedanken, A. Ultrasound-Assisted Polyol Method for the Preparation of SBA-15-Supported Ruthenium Nanoparticles and the Study of Their Catalytic Activity on the Partial Oxidation of Methane. *Langmuir* **2004**, *20*, 8352−8356.

(3) Graf, C.; van Blaaderen, A. Metallodielectric Colloidal Core−Shell Particles for Photonic Applications. *Langmuir* **2002**, *18*, 524−534.

(4) Liang, Z. J.; Susha, A.; Caruso, F. Gold Nanoparticle-Based Core-Shell and Hollow Spheres and Ordered Assemblies Thereof. *Chem. Mater.* **2003**, *15*, 3176−3183.

(5) Tessier, P. M.; Velev, O. D.; Kalambur, A. T.; Rabolt, J. F.; Lenhoff, A. M.; Kaler, E. W. Assembly of Gold Nanostructured Films Templated by Colloidal Crystals and Use in Surface-Enhanced Raman Spectroscopy. *J. Am. Chem. Soc.* **2000**, *122*, 9554−9555.

(6) Kubo, S.; Gu, Z. Z.; Tryk, D. A.; Ohko, Y.; Sato, O.; Fujishima, A. Metal-Coated Colloidal Crystal Film as Surface-Enhanced Raman Scattering Substrate. *Langmuir* **2002**, *18*, 5043−5046.

(7) Jiang, C. Y.; Markutsya, S.; Pikus, Y.; Tsukruk, V. V. Freely Suspended Nanocomposite Membranes as Highly-Sensitive Sensors. *Nat. Mater.* **2004**, *3*, 721−728.

(8) Gu, Z. Z.; Horie, R.; Kubo, S.; Yamada, Y.; Fujishima, A.; Sato, O. Fabrication of a Metal-Coated Three-Dimensionally Ordered Macroporous Film and Its Application as a Refractive Index Sensor. *Angew. Chem., Int. Ed.* **2002**, *41*, 1154−1156.

(9) Vanmaekelbergh, D. Self-Assembly of Colloidal Nanocrystals as Route to Novel Classes of Nanostructured Materials. *Nano Today* **2011**, *6*, 419−437.

(10) Li, F.; Josephson, D. P.; Stein, A. Colloidal Assembly: The Road from Particles to Colloidal Molecules and Crystals. *Angew. Chem., Int. Ed.* **2011**, *50*, 360−388.

(11) Vigderman, L.; Khanal, B. P.; Zubarev, E. R. Functional Gold Nanorods: Synthesis, Self-Assembly, and Sensing Applications. *Adv. Mater.* **2012**, *24*, 4811−4841.

(12) Yu, Q.; Huang, H.; Peng, X.; Ye, Z. Ultrathin Free-Standing Close-Packed Gold Nanoparticle Films: Conductivity and Raman Scattering Enhancement. *Nanoscale* **2011**, *3*, 3868−3875.

(13) Ming, T.; Kou, X.; Chen, H.; Wang, T.; Tam, H. L.; Cheah, K. W.; Chen, J. Y.; Wang, J. Ordered Gold Nanostructure Assemblies Formed by Droplet Evaporation. *Angew. Chem., Int. Ed.* **2008**, *47*, 9685−9690.

(14) Ahmed, S.; Ryan, K. M. Close-Packed Gold-Nanocrystal Assemblies Deposited with Complete Selectivity into Lithographic Trenches. *Adv. Mater.* **2008**, *20*, 4745−4750.

(15) Ahmed, S.; Barrett, C. A.; O'Sullivan, C.; Sanyal, A.; Geaney, H.; Singh, A.; Gunning, R. D.; Ryan, K. M. Electrophoretic Deposition of Spherical and Rod-Shaped Nanocrystals into Close Packed Superlattices. *ECS Trans.* **2009**, *19*, 209−219.

(16) Ahmed, S.; Ryan, K. M. Centimetre Scale Assembly of Vertically Aligned and Close Packed Semiconductor Nanorods from Solution. *Chem. Commun.* **2009**, 6421−6423.

(17) Liang, Z. J.; Susha, A.; Caruso, F. Metallodielectric Opals from Layer-by-Layer Processed Coated Colloids. *Adv. Mater.* **2002**, *14*, 1160−1164.

(18) Lu, L.; Randjelovic, I.; Capek, R.; Gaponik, N.; Yang, J.; Zhang, H.; Eychmüller, A. Controlled Fabrication of Gold-Coated 3D Ordered Colloidal Crystal Films and Their Application in Surface-Enhanced Raman Spectroscopy. *Chem. Mater.* **2005**, *17*, 5731−5736.

(19) Lu, L.; Eychmüller, A. Ordered Macroporous Bimetallic Nanostructures: Design, Characterization, And Applications. *Acc. Chem. Res.* **2008**, *41*, 244−253.

(20) Jiang, P.; Bertone, J. F.; Hwang, K. S.; Colvin, V. L. Single-Crystal Colloidal Multilayers of Controlled Thickness. *Chem. Mater.* **1999**, *11*, 2132−2140.

(21) Afonso, C. A. M.; Crespo, J. G. Recent Advances in Chiral Resolution through Membrane-Based Approaches. *Angew. Chem., Int. Ed.* **2004**, *43*, 5293−5295.

(22) van Reis, R.; Zydney, A. Bioprocess Membrane Technology. *J. Membr. Sci.* **2007**, *297*, 16−50.

(23) Ulbricht, M. Advanced Functional Polymer Membranes. *Polymer* **2006**, *47*, 2217−2262.

(24) Kallus, S.; Condre, J.-M.; Hahn, A.; Golemme, G.; Algieri, C.; Dieudonne, P.; Timmins, P.; Ramsay, J. D. F. Colloidal Zeolites and Zeolite Membranes. *J. Mater. Chem.* **2002**, *12*, 3343−3350.

(25) Tong, H. D.; Jansen, H. V.; Gadgil, V. J.; Bostan, C. G.; Berenschot, C. G. E.; van Rijn, C. J. M.; Elwenspoek, M. Silicon Nitride Nanosieve Membrane. *Nano Lett.* **2004**, *4*, 283−287.

(26) Nicole, L.; Boissiere, C.; Grosso, D.; Quach, A.; Sanchez, C. *J. Mater. Chem.* **2005**, *15*, 3598.

(27) Toh, C.-S.; Kayes, B. M.; Nemanick, E. J.; Lewis, N. S. Fabrication of Free-Standing Nanoscale Alumina Membranes with Controllable Pore Aspect Ratios. *Nano Lett.* **2004**, *4*, 767−770.

(28) Yamaguchi, A.; Uejo, F.; Yoda, T.; Uchida, T.; Tanamura, Y.; Yamashita, T.; Teramae, N. Self-Assembly of a Silica-Surfactant Nanocomposite in a Porous Alumina Membrane. *Nat. Mater.* **2004**, *3*, 337−341.

(29) Hinds, B. J.; Chopra, N.; Rantell, T.; Andrews, R.; Gavalas, V.; Bachas, L. G. Aligned Multiwalled Carbon Nanotube Membranes. *Science* **2004**, *303*, 62−65.

(30) Miller, S. A.; Martin, C. R. Redox Modulation of Electroosmotic Flow in a Carbon Nanotube Membrane. *J. Am. Chem. Soc.* **2004**, *126*, 6226−6227.

(31) Striemer, C. C.; Thomas R. Gaborski, T. R.; McGrath, J. L.; Fauchet, P. M. Charge- and Size-Based Separation of Macromolecules Using Ultrathin Silicon Membranes. *Nature* **2007**, *445*, 749−753.

(32) McPhie, P. Dialysis. *Methods Enzymol.* **1971**, *22*, 23−33.

(33) Bohaty, A. K.; Smith, J. J.; Zharov, I. Free-Standing Silica Colloidal Nanoporous Membranes. *Langmuir* **2009**, *25*, 3096−3101.

(34) Ignacio-de Leon, P. A.; Zharov, I. Size-Selective Transport in Colloidal Nano-Frits. *Chem. Commun.* **2011**, *47*, 553−555.

(35) Schepelina, O.; Poth, N.; Zharov, I. pH-Responsive Nanoporous Silica Colloidal Membranes. *Adv. Funct. Mater.* **2010**, *20*, 1962−1969.
(36) Lee, S. B.; Martin, C. R. pH-Switchable, Ion-Permselective Gold Nanotubule Membranes Based on Chemisorbed Cysteine. *Anal. Chem.* **2001**, *73*, 768−775.
(37) Hou, Z.; Abbott, N. L.; Stroeve, P. Self-Assembled Monolayers on Electroless Gold Impart pH-Responsive Transport of Ions in Porous Membranes. *Langmuir* **2000**, *16*, 2401−2404.
(38) Chun, K. Y.; Mafé, S.; Ramírez, P.; Stroeve, P. Protein Transport through Gold-Coated, Charged Nanopores: Effects of Applied Voltage. *Chem. Phys. Lett.* **2006**, *418*, 561−564.
(39) Asandei, A.; Pintilie, F.; Luchian, T. Transport and Kinetic Features of Gold-Functionalized Artificial Nanopores. *Romanian J. Biophys.* **2006**, *16*, 273−281.
(40) Velleman, L.; Shapter, J. G.; Losic, D. Gold Nanotube Membranes Functionalised with Fluorinated Thiols for Selective Molecular Transport. *J. Membr. Sci.* **2009**, *328*, 121−126.
(41) Hulteen, J. C.; Jirage, K. B.; Martin, C. R. Introducing Chemical Transport Selectivity into Gold Nanotubule Membranes. *J. Am. Chem. Soc.* **1998**, *120*, 6603−6604.
(42) Smuleac, V.; Butterfield, D. A.; Bhattacharyya, D. Permeability and Separation Characteristics of Polypeptide-Functionalized Polycarbonate Track-Etched Membranes. *Chem. Mater.* **2004**, *16*, 2762−2771.
(43) Zhang, H.; Ito, Y. pH Control of Transport through a Porous Membrane Self-Assembled with a Poly(acrylic acid) Loop Brush. *Langmuir* **2001**, *17*, 8336−8340.
(44) Lobbicke, R.; Chanana, M.; Schlaad, H.; Pilz-Allen, C.; Gunter, C.; Mohwald, H.; Taubert, A. Polymer Brush Controlled Bioinspired Calcium Phosphate Mineralization and Bone Cell Growth. *Biomacromolecules* **2011**, *12*, 3753−3760.
(45) Lokuge, I.; Wang, X.; Bohn, P. W. Temperature Controlled Flow Switching in ... Grafted by Atom Transfer Radical Polymerization. *Langmuir* **2007**, *23*, 305−311.
(46) Yu, S.; Lee, S. B.; Kang, M.; Martin, C. R. Size-Based Protein Separations in Poly(ethylene glycol)-Derivatized Gold Nanotubule Membranes. *Nano Lett.* **2001**, *1*, 495−498.
(47) Stöber, W.; Fink, A.; Bohn, E. Controlled Growth of Monodisperse Silica Spheres in the Micron Size Range. *J. Colloid Interface Sci.* **1968**, *26*, 62−69.
(48) Wang, W.; Gu, B.; Liang, L.; Hamilton, W. Fabrication of Two- and Three-Dimensional Silica Nanocolloidal Particle Arrays. *J. Phys. Chem. B* **2003**, *107*, 3400−3404.
(49) Le, T. V.; Ross, E. E.; Velarde, T. R. C.; Legg, M. A.; Wirth, M. J. Sintered Silica Colloidal Crystals with Fully Hydroxylated Surfaces. *Langmuir* **2007**, *23*, 8554−8559.
(50) Chabanov, A. A.; Jun, Y.; Norris, D. J. Avoiding Cracks in Self-Assembled Photonic Band-Gap Crystals. *Appl. Phys. Lett.* **2004**, *84*, 3573−3575.
(51) Zheng, S.; Ross, E.; Legg, M. A.; Wirth, M. High-Speed Electroseparations Inside Silica Colloidal Crystals. J. *J. Am. Chem. Soc.* **2006**, *128*, 9016−9017.
(52) Shah, R. R.; Merreceyes, D.; Husemann, M.; Rees, I.; Abbott, N. L.; Hawker, C. J.; Hedrick, J. L. Using Atom Transfer Radical Polymerization to Amplify Monolayers of Initiators Patterned by Microcontact Printing into Polymer Brushes for Pattern Transfer. *Macromolecules* **2000**, *33*, 597−605.
(53) Dong, R.; Lindau, M.; Ober, C. K. Dissociation Behavior of Weak Polyelectrolyte Brushes on a Planar Surface. *Langmuir* **2009**, *25*, 4774−4779.
(54) Tan, B. J. Y.; Sow, C. H.; Koh, T. S.; Chin, K. C.; Wee, A. T. S.; Ong, C. K. Fabrication of Size-Tunable Gold Nanoparticles Array with Nanosphere Lithography, Reactive Ion Etching, and Thermal Annealing. *J. Phys. Chem. B* **2005**, *109*, 11100−11109.
(55) Cussler, E. L. *Diffusion: Mass Transfer in Fluid Systems*, 2nd ed.; Cambridge University Press: New York, 1997.
(56) Advincula, R. C., Brittain, W. J., Caster, K. C., Rühe, J., Eds.; *Polymer Brushes: Synthesis, Characterization, Applications*; Wiley-VCH: Berlin, 2004.
(57) Biesalski, M.; Johannsmann, D.; Rühe, J. Synthesis and Swelling Behavior of a Weak Polyacid Brush. *J. Chem. Phys.* **2002**, *117*, 4988−4995.
(58) Kim, B.; Lim, S. H.; Ryoo, W. Preparation and Characterization of pH-Sensitive Anionic Hydrogel Microparticles for Oral Protein-Delivery Applications. *J. Biomater. Sci.* **2009**, *20*, 427−436.
(59) Schepelina, O.; Zharov, I. Poly(2-(dimethylamino)ethyl methacrylate)-Modified Nanoporous Colloidal Films with pH and Ion Response. *Langmuir* **2008**, *24*, 14188−14194.
(60) Schepelina, O.; Zharov, I. PNIPAAM-Modified Nanoporous Colloidal Films with Positive and Negative Temperature Gating. *Langmuir* **2007**, *23*, 12704−12709.